ELSEVIER

Journal of Chromatography A, 886 (2000) 9–18

JOURNAL OF CHROMATOGRAPHY A

www.elsevier.com/locate/chroma

On-column refractive index detector for flash chromatography

Sarah G. Westerbuhr, Kathy L. Rowlen*

Department of Chemistry and Biochemistry, University of Colorado, Boulder, CO 80309, USA

Received 20 December 1999; received in revised form 17 April 2000; accepted 17 April 2000

Abstract

A universal detector for on-column analysis in flash chromatography is reported. The detection scheme takes advantage of refractive index changes as analytes move through an illuminated region of the column. The column packing material is a diffuse scattering medium when the refractive index of the solvent is significantly different than that of the packing material. The magnitude of the 'signal' depends on the degree to which the refractive index mismatch is changed. An empirical model that qualitatively accounts for the observed trends is presented. This detection scheme provides a simple, inexpensive means to monitor the end of a flash chromatography column in order to determine the exit time of the species of interest, thus greatly reducing the post-column analysis time. Additionally, the detector is movable along the length of the column, offering the potential to monitor separations as they occur.

Keywords: Flash chromatography; Refractive index detection

1. Introduction

Flash and gravity-fed chromatography are simple, commonly used preparative techniques for the separation of reaction mixtures. The glass column containing the packing material allows for visualization of colored compounds as they are eluted from the column. However, because most separations involve non-colored compounds, products are typically isolated and identified by collecting and analyzing (post-column) numerous fractions of eluent. Post-column analysis usually involves tedious evaluation of often more than a dozen fractions by thin-layer chromatography. A universal detection method for flash chromatography that could be used to monitor the end of the column would provide the operator with the information necessary to collect only fractions that contain compounds of interest. In order to be useful to a wide range of practitioners of flash chromatography, the detector must also be inexpensive, easily portable, simple to use and versatile in terms of column size and separation conditions. For flash chromatography, sensitivity is generally not a critical issue since most samples are greater than mg quantities.

The packing materials for flash column chromatography are particles of silica gel or alumina which are large enough to efficiently scatter visible light; a typical particle size for silica gel is 60–200 mesh, or 75–250 μm diameter. The magnitude and direction of scattering depend upon the refractive indices of the particles and the surrounding solution, as well as roughness features of the surfaces of the particles [1]. Consequently, the extent of light scattering

*Corresponding author. Tel.: +1-303-492-1143; fax: +1-303-492-5894.

E-mail address: rowlen@spot.colorado.edu (K.L. Rowlen)

0021-9673/00/$ – see front matter
PII: S0021-9673(00)00488-X

through a packed column can be monitored to detect analytes; the magnitude of the signal is related to the degree to which the refractive index of the analyte matches that of the packing material. For example, if the refractive index of the analyte exactly matches the refractive index of the particles, non-absorbing particles become 'transparent'. In such a case, a non-absorbed light beam travels directly through the column (see Fig. 1B). Conversely, if the refractive index of the analyte is significantly different than that of the particles, the light beam is diffusely scattered (see Fig. 1A). Since the signal is dependent primarily on the analyte's refractive index, a detector based on this approach is nearly universal. The Christiansen refractive index detector for liquid chromatography is based on a similar effect [2,3]. However, the use of the Christiansen effect detector requires that the solvent refractive index identically match the refractive index of the particles at the particular wavelength of light used. The detector presented in this work does not have such a restriction.

The on-column refractive index instrument reported here is simple, inexpensive and mounts directly onto the glass column with brackets whose size can be easily varied. The instrument can be positioned at various points along the column to monitor the separation. For example, column efficiency [4], capacity factors [5], and boundary profiles [6–8] have been studied using multiple point on-column detection. Additionally, viscous fingering [9], solute migration [10], and sample introduction [11] have been studied by photographing a column where the refractive index of the solution matches that of the packing material and the refractive index of the analyte is significantly different from that of the packing material. Universal on-column detection for preparative chromatography offers additional

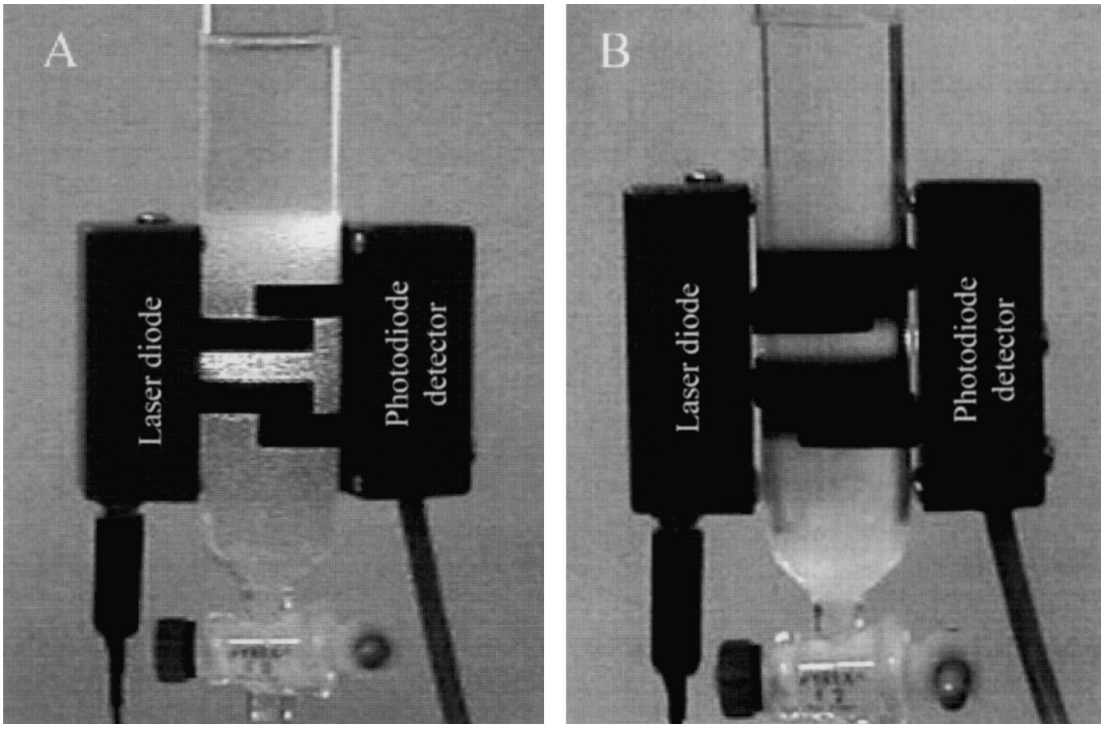

Fig. 1. Digital photograph of the instrument mounted onto a glass column packed with silica particles; the laser is contained in the box on the left side of each image, and the detector is in the box on the right. In (A) the solvent is water ($n_s = 1.333$), which leads to diffuse scattering of the beam. In (B) the solvent is chloroform ($n_s = 1.446$), which leads to forward scattering (in fact only a small portion of light scattered at the glass interface can be seen on the right side of the column).

advantages, including the potential for automation of fraction collection.

2. Experimental

2.1. Apparatus

A digital image of the instrument is shown in Fig. 1. The instrument consists of a diode laser light source, a photodiode detector, an analog-to-digital converter, and two light-weight power supplies. For this study a personal computer was employed for data collection, but a simple microprocessor/display could also be used. The long (3 ft) power/signal cables allow the source and detector to be placed inside a fume hood.

The light source was a laser diode with maximum emission at 660 nm and maximum power of 5 mW (Model #M6605 from NVG, Hazlehurst, GA, USA) with a 3.3-V (±5%) power supply. A 660-nm laser diode source was chosen because it is inexpensive, light weight, and the wavelength is not likely to be absorbed by most organic molecules. However, any wavelength that is not strongly absorbed by either the column or the packing material could be used. The laser was housed in an anodized aluminum box of dimensions 2.8×2.2×5.6 cm. The compartment had a 0.2-cm diameter aperture, allowing the entire beam to be transmitted to the column. A second compartment, with dimensions identical to the laser compartment, contained the photodiode detector (Model #S1226-8BK, Hamamatsu, Bridgewater, NJ, USA, 5 V±5% reverse bias). A 0.06-cm diameter aperture in the detector compartment was used to minimize background light at the photodiode. A cut-off filter between the detector compartment and column was also utilized to reduce background light. The filter allowed less than 0.1% transmission at 200–600 nm and 82.8% transmission at 660 nm.

The laser and detector compartments were mounted onto the glass column with metal clips (which can be made at the appropriate size). The clips permitted the laser and detector compartments to be rotated around the column relative to each other and allowed both compartments to be moved up and down the length of the column. The light source and detector could thus be positioned at right angles to each other (90° geometry), opposed to each other (180° geometry), and several angles between. A commercially available analog-to-digital converter (Blue Earth Micro 485, Blue Earth Research, Mankato, MN, USA) was used as an interface to a personal computer.

A short (10 cm) 2.5-cm diameter glass column with a Teflon stopcock was used as a representative flash column. The column is limited to materials that are transparent to the wavelength of light used. The column was packed with silica gel (60–200 mesh, Mallinckrodt, Paris, KY, USA) supported on a plug of glass wool at the stopcock. Compressed air was used to force solvent through the column.

2.2. Reagents

Ethyl acetoacetate (99+%) was obtained from Aldrich (Milwaukee, WI, USA), and salicylic acid (Reagent Grade) was obtained from Matheson, Coleman, & Bell. Technical-grade nickel chloride hexahydrate ($NiCl_2 \cdot 6H_2O$) was purchased from Fisher Scientific (Fair Lawn, NJ, USA). All other chemicals were ACS certified and obtained from Fisher Scientific (Pittsburgh, PA, USA), with the exception of distilled water.

2.3. Procedures

For the solvent-based studies, a solvent was flushed through the packed column until a constant baseline was obtained, at which point the solvent was considered to be equilibrated with the column. An acceptable baseline exhibited a drift of ≤1% over a 5-min period and noise of ≤±3 mV. The magnitude of the baseline signal depended on such parameters as the solvent used and the source/detector geometry. The magnitude of the signal was measured with the detector at 90 and 180°, and at 10° intervals between 90 and 180°.

For calibration of the instrument response as a function of analyte concentration, the column was first equilibrated with the indicated solvent, a known volume of solution (analyte dissolved in solvent) was deposited at the top of the column and the analyte was subsequently eluted with the solvent. Based on the volume used and the concentration of the analyte in solution, the total mass of analyte deposited on the

column was calculated. For the case of ethyl acetoacetate eluted with methanol, a known volume of pure liquid analyte was added to the top of the column. The mass of ethyl acetoacetate added was calculated from its density. Nickel chloride hexahydrate ($NiCl_2 \cdot 6H_20$) was chosen as a model absorbing analyte. A 0.25 *M* solution in water had an absorbance of 0.4552 at 660 nm (1 cm pathlength). Absorbance measurements were made with an HP model 8452A Diode Array Spectrometer (Hewlett-Packard, Wilmington, DE, USA).

For the measurements made with the on-column refractive index detector, the detection unit was positioned approximately 6 cm from the top of the column unless otherwise stated. This position was arbitrarily chosen; the detector unit may be positioned at any point along the length of the column. Although not always true for flash chromatography, it was noted that for the amounts of analyte loaded onto the column in this study, the peaks were generally Gaussian in shape. Therefore, peak areas and heights were obtained from Gaussian fits to the data using GRAMS/32 (ver. 4.01, Galactic Industries, Salem, NH, USA).

The photodiode response (signal as a function of mW at the detector) was calibrated by attenuating the beam to varying degrees through solutions of an absorbing dye (green food coloring) placed in a cuvette. The detector signal in mV was measured as a function of the percent transmission (%*T*) for each solution. The amount of light reaching the detector was then estimated from the power of the laser, the %*T* of the solution, the laser spot size (assuming uniform intensity), the amount of light lost at the glass cuvette surfaces (4% per surface), and the detector aperture size.

3. Results and discussion

3.1. Chromatography (application)

As can be observed in Fig. 1A, the light beam is diffusely scattered by the packing material. The amount of light exiting the column at any angle from the source direction is dependent on the refractive index of both the packing material and the solution. In order to determine the excitation/detection geometry that resulted in the largest change in signal for a given mismatch in refractive index, various solvents were flushed through the column and the signal monitored at different angles between the source and detector. Specifically, the detector and laser were positioned in either a 90 or a 180° geometry for nine different solvents. The 180° geometry was found to be more sensitive to changes in the solvent refractive index. As an example, the change in signal when the solvent was switched from ethyl acetate to methanol is shown in Fig. 2. The detector signal decreases by ~300 mV as methanol displaces ethyl acetate in the column. This behavior can be rationalized by considering that the refractive index of ethyl acetate (n_s = 1.370, where n_s designates the refractive index of the solvent) more closely matches that of the silica (n_p ~1.55, where n_p designates the refractive index of the packing material) than the refractive index of methanol (n_s = 1.326) does. Note that the reported refractive indices (n_D) are strictly valid only at 589.32 nm [12]. However, the refractive indices at the wavelength of interest here (660 nm) should be very similar to n_D. For example, the refractive indices for water [13] and chloroform [14] at 660 nm differ from those at 589 nm by less than 0.5%.

The smooth transition observed in Fig. 2 also demonstrates the ease with which a step-wise solvent gradient could be used. In contrast to the trend observed when the solvent is switched, Fig. 3 shows

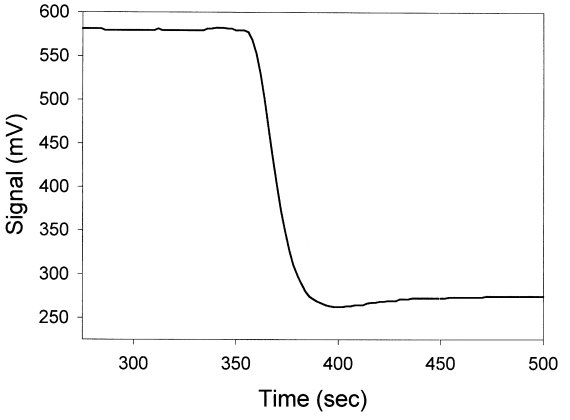

Fig. 2. The instrument response (for the 180° geometry shown in Fig. 1) to changing the solvent from ethyl acetate (n_s = 1.370) to methanol (n_s = 1.326). In this case the signal is defined as the baseline voltage achieved once the column is equilibrated with solvent.

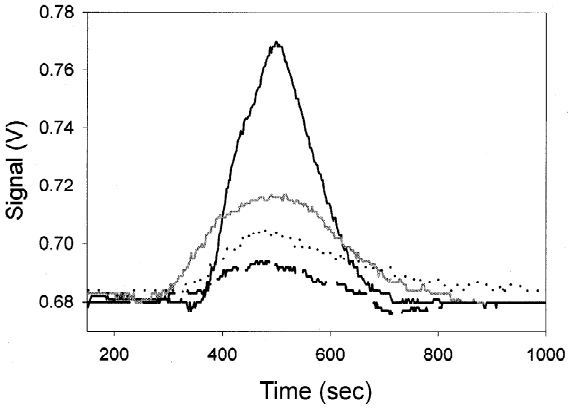

Fig. 3. Sample chromatograms for ethyl acetoacetate eluted with ethyl acetate. Each has been shifted to an arbitrary time for the signal maximum. The various curves correspond to different quantities of ethyl acetoacetate added to the top of the column (ranging from 102 to 510 mg).

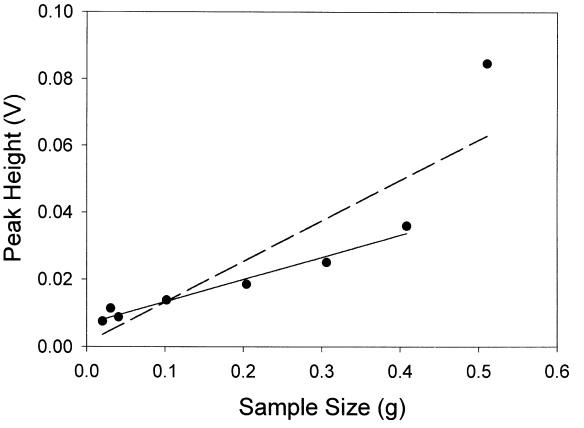

Fig. 4. Calibration curve for the analyte ethyl acetoactate eluted with ethyl acetate. The dotted line is the linear regression for all of the data points shown in the figure. The solid line is the linear regression excluding the data point for 0.51 g.

the transient peak for a non-absorbing analyte as it passed through the detection zone (with the source and detector in the 180° geometry). As expected for flash chromatography, the peaks are broad. However, the analyte band is clearly distinguishable from a transition in the solvent. Thus, a step-wise gradient could be used in conjunction with the detector by noting movement of the analyte band before and after the new solvent front has moved past the detection zone.

In order to determine the concentration response, the peak height was measured as a function of analyte mass (monitored at the same position on the column and therefore in the same volume [4]). The calibration curve for the analyte ethyl acetoacetate eluted with ethyl acetate is shown in Fig. 4, as an example. The calibration curves (summarized in Table 1) are reasonably linear at the lower mass ranges investigated but do exhibit a slight degree of curvature for higher sample masses. As discussed in detail later, the sensitivity (change in signal as a function of change in analyte concentration) is dependent on the refractive index of all three components and may therefore be specified for only a particular system. The lowest detected amounts in this study are summarized in Table 1. The calculated limit of detection for the specific non-absorbing compounds investigated with this particular, un-optimized instrument (5 mW source, 2.5 cm dia. silica-packed column) is approximately 45 mg. It is anticipated that tens of mg is a representative number since the solvents used in this study are commonly used for flash chromatography and the analytes were representative. The limit of detection could be significantly improved by optimization of detector sensitivity. For the estimated light flux regime used in these studies the photodiode had a response of ~0.7 V/μW of laser power reaching the detector. For comparison, at higher light fluxes the detector exhibited a response of ~4 V/μW.

The 180° source/detector geometry also functions as an absorbance detector. The chromatographic peaks for an absorbing compound, $NiCl_2 \cdot 6H_20$, are shown in Fig. 5. In this case, the signal reaching the detector (in the 180° geometry) decreased due to absorption of the light beam. This figure also demonstrates another feature of the detection scheme: the detector may be positioned at any point along the length of the column. As expected, near the top of the column the peak width is narrower than near the bottom. In addition, the progress of the separation may be monitored by periodically repositioning the detection unit.

In order to quantify the amount of light that actually passed through the center of the column and not around the glass edges, another highly absorbing green dye was used. Specifically, a 5.0-ml volume of an optically thick dye (green food coloring) was

Table 1
Summary of analyte response data[a]

Analyte	n_a	Solvent	n_s	Mass range (mg)	Slope$\pm\sigma$	y-Intercept$\pm\sigma$	R	LOD (mg)	LDA (mg)	S/N
Salicylic acid	1.565	Ethyl acetate	1.370	14–240	0.47±0.06	0.011±0.007	0.973	45	14	7
Ethyl acetoacetate	1.419	Ethyl acetate	1.370	20–510	0.12±0.02	0.001±0.007	0.887	175	20	4.2
					0.066±0.005[b]	0.007±0.001	0.984	45		
Ethyl acetoacetate	1.419	Methanol	1.326	20–1020	0.088±0.006[c]	0.004±0.002	0.978	68	20	2.5
Nickel chloride	–	Water	1.333	2–60	1.7±0.2	0.01±0.01	0.954	18	2.4	2.5

[a] The symbol n_a is the analyte refractive index and n_s is the solvent refractive index. mass range is the range investigated. The slope is based on a linear regression to the signal versus grams data; the units of slope are V (peak height) per g of analyte. The units of the y-intercept are V (peak height). R is the correlation coefficient of the linear regression. The LOD is the limit of detection calculated as 3× the standard deviation of the intercept divided by the slope. LDA is the lowest detected amount, and S/N is the signal-to-noise ratio for the LDA based on peak height and half the peak-to-peak noise in the background. When peak area was used instead of peak height, the linear regression fits were poorer, but the trends were similar to those for peak height.

[b] Linear regression data when the highest concentration point is not included in fit (see Fig. 4).

[c] From the average of two independent data sets.

eluted through the column with water. The undiluted dye had a transmittance of 0.013 %T at 660 nm. The signal obtained with the dye moving through the detection zone was 9 mV. The dark noise was measured to be 7±1 mV; therefore only 2 mV can be attributed to light reaching the detector. Utilizing a calibration curve for the detector (signal as a function of mW at the detector), it was estimated that 2 mV corresponds to 0.4% of light reaching the detector without passing through the column for a typical 0.5 V signal. Therefore, it is unlikely that the signal is affected by light scattering around the glass edges rather than through the column bed.

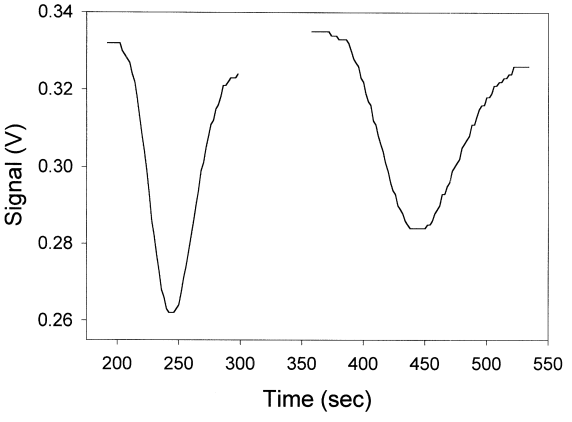

Fig. 5. Signal for 120 mg of $NiCl_2 \cdot 6H_20$ (%$T \approx 3\%$) eluted with water. The inverted peak on the left was monitored with the source/detector positioned 2 cm from the top of the column and the inverted peak on the right with the source/detector positioned at 6 cm from the top.

Other issues relevant to accurate detection of analyte peaks, such as temperature and pressure effects on refractive index, were also addressed. It is well known that the primary limit to sensitive detection in standard refractive index detectors is thermal fluctuations which lead to fluctuations in the refractive index. The general rule is that the refractive index of an organic liquid changes by 4×10^{-4} units per degree [15]. Since the instrument presented here was designed for relatively high quantities of analyte (mg), normal laboratory temperature fluctuations were tolerable (i.e., no temperature control was necessary).

Flash chromatography typically utilizes compressed air to speed up the flow of solvent through the column. While there are fluctuations in the pressure applied to the column during the course of a separation, the magnitude of the these pressure fluctuations resulted in negligible changes in refractive index of the solvent (the coefficient is 4×10^{-5} per atmosphere [15]). However, the packing density of the stationary phase is more susceptible to changing pressure. We have noted that poorly packed columns, as determined by visual inspection, were sensitive to a change in pressure. For example, when the pressure was alternated between atmospheric and the maximum pressure (as determined by a forceful disjoining of the lid from the column), the signal permanently changed by as much as 11 mV. For a

visually well packed column, the signal spiked up to 11 mV when the air flow was first applied, but rapidly (~1 s) returned to the baseline signal (±3 mV). Compared to the 11-mV spike associated with an abrupt pressure change, the signal observed for an analyte near the limit of detection would have a similar change in the magnitude of the signal, but the peak would last at least 30 s. Therefore, pressure changes are not likely to yield false positive peak detection.

3.2. Scattering trends (theory)

In order to accurately describe the scattering process it would be necessary to have a quantitative measure of the distribution of the surface roughness feature sizes for a specified silica particle size [1]. In addition, the silica gel used here has a wide range of particle sizes. It would also be necessary to quantify the angular distribution function of the scattered light as a function of solvent refractive index. Considering that the envisioned application of this instrument is qualitative identification of analyte exit time from a column, the sophisticated studies required to fully characterize the system were not undertaken. However, studies were conducted in order to better understand the observed trends in signal as a function of solvent/analyte refractive index. From these studies it was possible to develop an empirical model that qualitatively describes the observed trends.

Fig. 6 shows the measured trend in signal as a function of refractive index mismatch (defined as the difference in n_D for the silica and solvent) for both the 90 and 180° geometries. As the refractive index of the solvent approached that of the silica, the signal for the 90° geometry decreased slightly while the signal for the 180° geometry increased dramatically. Based on the observed trend for the 180° geometry (transmission geometry), and because of the small aperture on the detector (i.e., small acceptance angle), it is postulated that the transmission axis may be qualitatively treated as in the Beer-Lambert law, where the attenuation of light at the detector is related to an effective scattering cross-section (σ_{scat}) in the column. Since the particle sizes in this case are large with respect to the excitation wavelength, it is proposed that the effective scattering cross-section

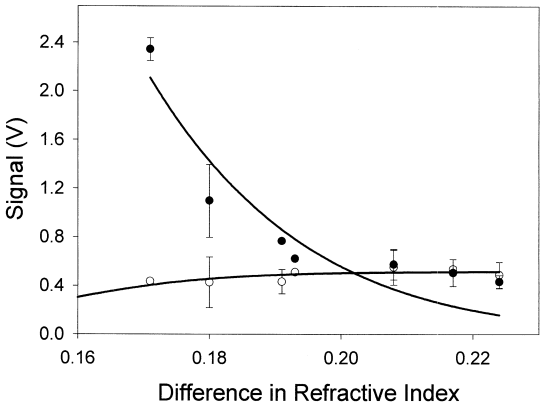

Fig. 6. The instrument signal as a function of $n_p - n_s$ for the 90° geometry (open circles) and the 180° geometry (filled circles). The fit to the 180° geometry data is given by Eq. (2). The R value is 0.94 and the values for P_o and k are 78±70 and 124±28, respectively. The line for the 90° geometry is only a guide to the eye. The seven data points, from left-to-right, correspond to the following solvents: hexanes, ethyl acetate, ethanol, acetone, acetonitrile, water and methanol. Two additional solvents, chloroform and ethyl acetoacetate matched the packing material's refractive index well enough to saturate the detector.

may be approximated using the Fresnel equation for normal incidence and specular reflection:

$$\sigma_{scat} \propto \left(\frac{n_p - n_s}{n_p + n_s} \right)^2 \quad (1)$$

where n_p is the packing material refractive index and n_s is the solvent refractive index. Thus, the magnitude of the signal (P) at 180° is:

$$P \approx P_o \, e^{-k(n_p - n_s)^2} \quad (2)$$

where P_o is a measure of the detected power in the absence of packing material and k is an experimental constant. The value of $1/(n_p + n_s)^2$ is approximated to be constant and is included in k; this approximation is not necessary but is reasonable in light of other factors which limit the application of the model. For example, the model assumes that the pathlength remains constant as the solvent refractive index changes. However, the pathlength undoubtedly changes as the system switches between an essentially transparent medium to a diffusely scattering medium. Even with such a caveat, the model is intuitively satisfying. If the refractive index of the packing material is equal to the refractive index of

the solvent ($n_p = n_s$), the signal is equal to a constant (P_o). As the difference in refractive indices increases, the signal decreases—as observed. While the fit of the raw data (in Fig. 6) to Eq. (2) is not superb, it is in qualitative agreement.

The data in Fig. 6 suggest two specific scattering regimes: one in which the refractive index mismatch is large and the particles are a diffusely scattering, or Lambert [1], surface, and another in which the refractive index mismatch is small and light is scattered primarily in the forward direction. These extreme cases are demonstrated in Fig. 1; the solvent in (A) is water ($n_s = 1.333$) and the solvent in (B) is chloroform ($n_s = 1.446$). One would predict an intermediate case in which the light is scattered nearly isotropically. Further evidence for the transition between two distinct scattering conditions, diffuse and forward, was obtained by probing the angular dependence of the scattering signal. By systematically varying the angle between the source and detector (between 90 and 180°), the angular dependence of scattering was mapped out for three solvents, water, acetonitrile, and ethyl acetate. As observed in Fig. 7, for the larger refractive index mismatch between the solvent and packing material (water as solvent, $n_s =$ 1.333) the detector signal is largest in the 90° geometry and decreases as the detector is positioned in the forward scattering direction. At an intermediate mismatch in refractive index (acetonitrile, $n_s = 1.342$) the signal is reasonably constant at all angles, suggesting isotropic scattering (at least in the forward hemisphere). With a better match between the solvent (ethyl acetate, $n_s = 1.370$) and packing material, the signal increases as the detector is moved from the 90 to the 180° geometry, suggesting primarily forward scattering. As indicated in both Figs. 6 and 7, the 'cross-over' refractive index for the two scattering conditions appears to be ~1.34. For this particular system, 1.34 is the solvent refractive index for which light is scattered equally at both 90 and 180° from the source. It is worth noting that the signal-to-noise ratio (based on the magnitude of the signal-to-rms noise in the background) is also better in the 180° geometry for ethyl acetate. For water and acetonitrile, the signal-to-noise ratio is independent of detector geometry over the range of 90–180°.

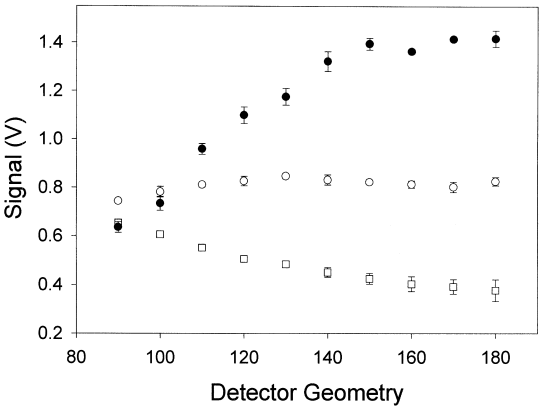

Fig. 7. The instrument signal as a function of the angle between the source and detector. The filled circles are for ethyl acetate ($n_s = 1.370$), open circles for acetonitrile ($n_s = 1.342$), and open squares for water ($n_s = 1.333$). The range for two measurements represents the variation due to repositioning the detector and laser compartments on the column. The average relative error associated with removal of the instrument and repacking the column is much higher (on the order of 20%). Such large error is associated with variables such as repacking the column, re-adjusting the source and detector, and variability in the laser power.

Further development of the model presented in Eq. (2) is necessary to treat the signal versus concentration data reported in Table 1. In this case, the signal varies in time and peak height (defined as the difference between the peak maximum and the baseline) is employed as the signal ($S_{s,a}$). Based on a difference measurement it is proposed that the signal maximum ($S_{s,a}$) may be approximated by:

$$S_{s,a} \approx P_o \left| e^{-k(n_p - n_s)^2} - e^{-k(n_p - n_{s,a})^2} \right| \quad (3)$$

where $n_{s,a}$ is the composite refractive index of the analyte and the solvent. The first term is a measure of the baseline magnitude (solvent as the mobile phase), and the second term is a measure of the combined effect of the analyte and solvent as the analyte moves through the detection zone. The absolute value is used for the purposes of comparing the signal magnitude as a function of analyte concentration (or volume). The composite refractive index of the analyte and solvent may be calculated from [15]:

$$n_{s,a} = n_s - n_s V_a + n_a V_a \quad (4)$$

where V_a is the volume of the analyte, V_s is the volume of the solvent, n_a is the refractive index of the analyte, and the total volume ($V_s + V_a$) is set equal to one, such that $V_s = 1 - V_a$.

Substituting Eq. (4) into Eq. (3), it is possible to predict the trends in signal as a function of refractive index differences and volume action of analyte. When the solvent and analyte have the same refractive index, intuitively one would predict that no signal should be observed. Evaluating Eq. (3) for $n_s = n_{s,a}$, the signal does indeed equal zero. In addition, for a given value of $n_p - n_s$, the equation satisfactorily predicts an increase in signal for an increase in the difference in solvent/analyte refractive indices. Using the constants obtained by fitting the data shown in Fig. 6 to Eq. (2), the model (Eq. (3)) was numerically evaluated. Fig. 8A shows the calculated trends for the case in which the refractive index of the particles is significantly different than the refractive index of the solvent (difference in refractive index of 0.22). This is the case that most closely matches the experimental conditions reported in this study. Note that the trend for analyte volume fractions less than 0.2 is reasonably linear, with the slope (and curvature) being greater for analyte refractive indices that best match that of the particles. These trends are in qualitative agreement with our experimental observations: reasonably linear signal versus volume (or mass) curves and better sensitivity for high refractive index analytes (see Table 1). Although the model can be made to fit the data, there are too many unknown parameters for a quantitative comparison (e.g., the exact expression for scattering angle distribution function, the volume of the analyte at any position on the column, etc.). However, if the refractive indices for the analyte–solvent–particles listed in Table 1 are used in the model, it is predicted that the salicylic acid–ethyl acetate combination on silica should have a response slope 17× that of the ethyl acetoacetate–methanol combination—a ratio of 5 is observed. Given the complexity of scattering in dense media, the qualitative agreement between the empirical model and experiment is deemed adequate.

The model was used to predict the trends for the case in which the solvent and particle refractive indices are nearly a perfect match (difference in refractive index of 0.05). The calculated results are shown in Fig. 8B. An example of this case would be chloroform as the solvent for a silica packing material (see Fig. 1B). It was not possible to experimentally investigate this regime using the current configuration of our apparatus due to saturation of the detector. Intuitively, one would expect the analyte to exert a much larger influence on the signal, since the system would switch between a nearly 100% forward scattering (or transmitted) condition, to one in which the packing material becomes highly scattering. The model shows just

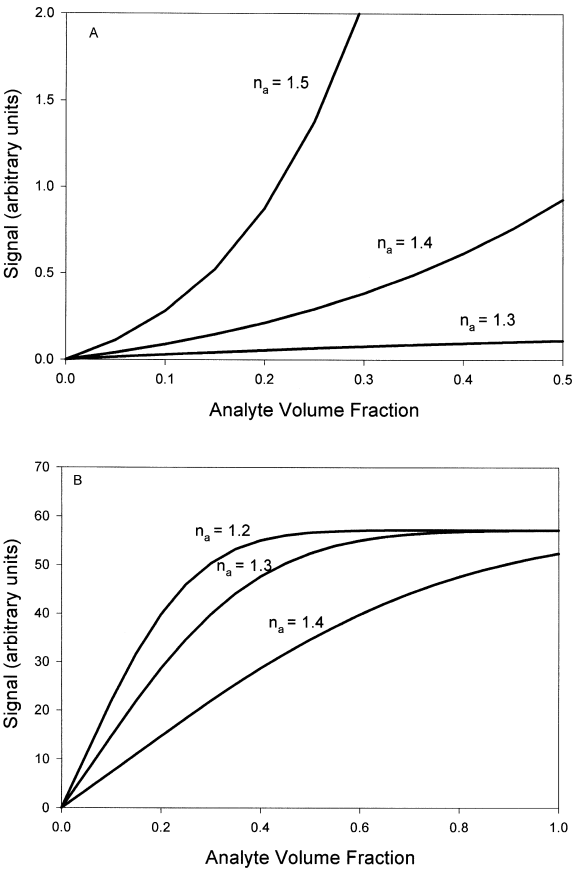

Fig. 8. Predicted (using Eq. (3)) signal ($S_{s,a}$) as a function of volume fraction of analyte on the column. The refractive index values used were $n_p = 1.55$, $n_s = 1.33$ in (A) and $n_p = 1.55$, $n_s = 1.50$ in (B).

such trends. Note that the signal magnitude for a given change in analyte volume is much larger than the case shown in Fig. 8A.

Acknowledgements

The authors gratefully acknowledge funding from the National Science Foundation.

References

[1] B. Hapke, in: Theory of Reflectance and Emittance Spectroscopy, Cambridge University Press, Cambridge, 1993.
[2] A.J.P. Martin, J.M. Miller, R.J. Mathieu, A.E. Lawson Jr., The Christiansen Effect Detector, US Patent 4042304, 1977.
[3] E.S. Yeung, in: E.S. Yeung (Ed.), Detectors for Liquid Chromatography, Wiley, New York, 1986, p. 18, Ch. 1.
[4] K.L. Rowlen, K.A. Duell, J.P. Avery, J.W. Birks Chem, Anal. Chem. 63 (1991) 575.
[5] K.L. Rowlen, K.A. Duell, J.P. Avery, J.W. Birks, Anal. Chem. 61 (1989) 2624.
[6] E.E. Brumbaugh, G.K. Ackers, J. Biol. Chem. 243 (1968) 6315.
[7] M.M. Jones, G.A. Harvey, G.K. Ackers, Biophys. Chem. 5 (1976) 327.
[8] J.R. Grothusen, J.K. Zimmerman, Biophys. Chem. 20 (1984) 299.
[9] B.S. Broyles, R.A. Shalliker, D.E. Cherrak, G. Guiochon, J. Chromatogr. A 822 (1998) 173.
[10] R.A. Shalliker, B.S. Broyles, G. Guiochon, J. Chromatogr. A 826 (1998) 1.
[11] B.S. Broyles, R.A. Shalliker, G. Guiochon, J. Chromatogr. A 855 (1999) 367.
[12] D.R. Lide (Ed.), CRC Handbook of Chemistry and Physics, 73rd Edition, CRC Press, Boca Raton, FL, 1992.
[13] P. Schiebener, J. Straub, J.M.H. Levelt Sengers, J.S. Gallagher, J. Phys. Chem. Ref. Data 19 (1990) 677.
[14] S. Valkai, J. Liszi, I. Szalai, J. Chem. Thermodyn. 30 (1998) 825.
[15] A. Braithwaite, F.J. Smith, in: Chromatographic Methods, 5th Edition, Blackie Academic and Professional, Glasgow, 1996, Ch. 6.